



# Exploring the signaling space of a GPCR using bivalent ligands with a rigid oligoproline backbone

Nina Romantini<sup>a</sup>, Shahidul Alam<sup>a,b</sup>, Stefanie Dobitz<sup>c</sup>, Martin Spillmann<sup>b</sup>, Martina De Foresta<sup>c</sup>, Roger Schibli<sup>a</sup>, Gebhard F. X. Schertler<sup>d</sup>, Helma Wennemers<sup>c</sup>, Xavier Deupi<sup>e,f</sup>, Martin Behe<sup>a</sup>, and Philipp Berger<sup>b,1</sup>

<sup>a</sup>Center for Radiopharmaceutical Sciences, Paul Scherrer Institute, CH-5232 Villigen, Switzerland; <sup>b</sup>Laboratory of Nanoscale Biology, Paul Scherrer Institute, CH-5232 Villigen, Switzerland; <sup>c</sup>Laboratory of Organic Chemistry, ETH Zürich, CH-8093 Zürich, Switzerland; <sup>d</sup>Department of Biology and Chemistry, Paul Scherrer Institute, CH-5232 Villigen, Switzerland; <sup>e</sup>Laboratory of Biomolecular Research, Paul Scherrer Institute, CH-5232 Villigen, Switzerland; and <sup>f</sup>Condensed Matter Theory Group, Paul Scherrer Institute, CH-5232 Villigen, Switzerland

Edited by Robert J. Lefkowitz, HHMI, Durham, NC, and approved October 27, 2021 (received for review May 11, 2021)

**G protein-coupled receptors (GPCRs) are one of the most important drug-target classes in pharmaceutical industry. Their diversity in signaling, which can be modulated with drugs, permits the design of more effective and better-tolerated therapeutics. In this work, we have used rigid oligoproline backbones to generate bivalent ligands for the gastrin-releasing peptide receptor (GRPR) with a fixed distance between their recognition motifs. This allows the stabilization of GPCR dimers irrespective of their physiological occurrence and relevance, thus expanding the space for medicinal chemistry. Specifically, we observed that compounds presenting agonists or antagonists at 20- and 30-Å distance induce GRPR dimerization. Furthermore, we found that 1) compounds with two agonists at 20- and 30-Å distance that induce dimer formation show bias toward Gq efficacy, 2) dimers with 20- and 30-Å distance have different potencies toward β-arrestin-1 and β-arrestin-2, and 3) the divalent agonistic ligand with 10-Å distance specifically reduces Gq potency without affecting β-arrestin recruitment, pointing toward an allosteric effect. In summary, we show that rigid oligoproline backbones represent a tool to develop ligands with biased GPCR signaling.**

G protein-coupled receptors | cell signaling | receptor dimerization

**G** protein-coupled receptors (GPCRs) comprise a wide and diverse family of seven-transmembrane helix proteins found in almost all eukaryotic organisms. GPCRs are essential in physiology, as they mediate cellular signaling inducing short-term effects and, in the long run, control cellular changes such as cell proliferation, differentiation, and migration. Therefore, GPCR malfunction is often translated into pathological outcomes (1). Currently, 108 GPCRs are targeted by 475 Food and Drug Administration-approved drugs, making them one of the most important pharmaceutical drug targets with around 25% of the prescribed drugs acting through this family of receptors (2). Initially, it was believed that GPCRs signaled independently from the type of ligand in a defined ratio through G-protein and arrestin pathways. However, certain natural and synthetic ligands are able to preferentially trigger a subset of these signaling pathways, a phenomenon designated as biased signaling, selective agonism, or collateral efficacy (3). Many GPCRs display such behavior, such as angiotensin, β-adrenergic, chemokine, and serotonin receptors (see ref. 4 for a comprehensive list). This raises interesting possibilities for the design of new therapeutics that target specific GPCR pathways (4). β-adrenergic receptors are one of the earliest and most studied models of biased signaling. In these receptors, agonists are used as bronchodilators for the treatment of obstructive pulmonary diseases (e.g., asthma), while antagonists (beta blockers) are used for the chronic treatment of heart failure. Interestingly, one of the antagonist beta blockers, carvedilol, can induce β-arrestin-1- and β-arrestin-2-mediated EGFR transactivation downstream of Erk activation (5). Carvedilol is therefore classified as a biased agonist, and it is unique

compared to typical beta blockers. Besides the clinically approved carvedilol, several potential biased drugs are in clinical or preclinical trials (6, 7).

While most GPCRs are able to function as monomers, there is clear evidence that dimerization (or even higher-order oligomerization) represents an additional layer of regulation and a fundamental aspect of receptor function (8). Nevertheless, GPCR oligomerization is still a controversially discussed field, probably because several modes of oligomerization exist. For example, the class C GPCRs GABA<sub>B1</sub> and GABA<sub>B2</sub> are linked together by a cytoplasmic coiled coil to form a functional GABA<sub>B</sub> receptor dimer, whereas 5-HT<sub>2A</sub> and mGluR2 interact through their transmembrane helices (9, 10). Crystal structures also point toward homodimerization based on transmembrane interactions. For instance, the μ-opioid receptor can dimerize through two different interfaces: a larger interface formed by transmembrane (TM) helices TM5 and TM6 and a smaller interface formed by TM1, TM2, and the intracellular helix 8 (11). The functional relevance of homo- and heterodimerization has been, in the meantime, shown for many other GPCRs (12, 13).

Homo- and heteromers can exhibit different pharmacology than monomers and, therefore, represent an obvious therapeutic target. Bivalent ligands for opioid receptors were already introduced in the 1980s before natural association of GPCRs was shown (14, 15). In the meantime, many bivalent ligands, especially for opioid and serotonin receptors, were synthesized.

## Significance

**G protein-coupled receptors (GPCRs) are major players in cellular signal transmission. In this work, we have used rigid oligoproline backbones derivatized with two ligands at defined distances to induce GPCR dimer formation as a way to alter its signaling profile. We show that bivalent ligands at distances of 20 and 30 Å induce dimers of the GRPR receptor with different signaling responses. In addition, a nondimer-inducing bivalent ligand (with 10-Å distance between agonists) also induces different signaling patterns, most likely due to allosteric effects. These findings identify bivalent ligands with a stiff oligoproline backbone as tools to explore the natural signaling space of GPCRs.**

Author contributions: N.R., S.A., H.W., M.B., and P.B. designed research; N.R., S.A., S.D., M.S., M.D.F., and P.B. performed research; S.D., M.S., M.D.F., R.S., G.F.X.S., H.W., M.B., and P.B. contributed new reagents/analytic tools; N.R., M.D.F., X.D., M.B., and P.B. analyzed data; and N.R., R.S., G.F.X.S., H.W., X.D., M.B., and P.B. wrote the paper.

The authors declare no competing interest.

This article is a PNAS Direct Submission.

This open access article is distributed under [Creative Commons Attribution-NonCommercial-NoDerivatives License 4.0 \(CC BY-NC-ND\)](https://creativecommons.org/licenses/by-nc-nd/4.0/).

<sup>1</sup>To whom correspondence may be addressed. Email: Philipp.Berger@psi.ch.

This article contains supporting information online at <http://www.pnas.org/lookup/suppl/doi:10.1073/pnas.2108776118/-DCSupplemental>.

Published November 22, 2021.

Critical factors in the development of these compounds are the length, rigidity, and water solubility of the linker. Most of the time, flexible linkers with a length of 18 to 25 atoms, corresponding to ~20- to 30-Å distance, have been used (reviewed, for example, in refs. 16 and 17).

Oligoprolines are conformationally well-defined molecular scaffolds that can be functionalized at defined sites to obtain bivalent ligands. Oligoproline derivatives are well soluble in water under physiological conditions and therefore ideally suited scaffolds for applications in aqueous media. In aqueous environments, oligoprolines adopt a highly symmetric polyproline II helix conformation in which every third residue is stacked on top of each other at a distance of ~10 Å (18). The functionalization pattern of this molecular scaffold can be easily fine-tuned by modular chemical synthesis reminiscent to an “LEGO” approach. In addition to their application for targeting GPCRs, oligoprolines have also shown their value in the development of inhibitors of protein–protein interactions, cell-penetrating peptides, hierarchical supramolecular assemblies, and the controlled formation of silver nanoparticles (19).

In this work, we use functionalized oligoproline backbones to induce artificial homodimers of the gastrin-releasing peptide receptor (GRPR) (now properly known as bombesin BB<sub>2</sub> receptor) to explore its signaling space. GRPR is a class-A GPCR that belongs to the bombesin family, and its homodimerization has not been documented so far. It is mainly expressed in different regions of the gastrointestinal (GI) tract and the brain (20, 21). GRPR does not only regulate various functions in the GI tract, such as gut hormone secretion and GI motility (22), but also many processes of the central nervous system like the regulation of memory, fear, and itching (23). Interestingly, GRPR was found to be overexpressed on different cancer types, among them prostate cancer and breast cancer, and its overexpression is accompanied by an ability to accelerate growth of cancer cells and increase their invasive potential (24, 25). Studies in tumor xenograft mouse models already showed that GRPR antagonists are able to decrease tumor growth rate (26), suggesting the interest of GRPR as a drug target. In addition, the specific delivery of radiolabeled peptides to tumor cells overexpressing the receptor enables targeted radiotherapy and nuclear imaging of these cancers.

Here, we show that bivalent oligoproline-based ligands with a distance of 20 and 30 Å between the recognition motifs are indeed able to induce dimerization of GRPR. The consequences for signaling of these changes in the oligomerization state were evaluated by measuring recruitment of six different adaptor proteins from three gene families (Gαq, β-arrestin-1/2, and GRK2/3/5). We show that dimerization can, indeed, influence the recruitment profile of GRPR, and we observe different recruitment efficacies and potencies of our tested drugs. In addition, we observed a strong effect on Gq recruitment of our bivalent ligand that was unable to induce dimerization, suggesting an allosteric effect.

## Results

**Ligands.** For our studies, we used divalent ligands consisting of oligoprolines as rigid scaffolds that allow for tailoring distances of 10, 20, and 30 Å between agonistic and/or antagonistic ligands. In particular, as recognition motifs, we used truncated derivatives of bombesin, such as the targeting motif from RM1 (27) as antagonist and the targeting motif from AMBA (28) as agonist, in which we replaced the C-terminal methionine with a norleucine. Our oligoproline backbones were modified with a 2,2',2'',2'''-(1,4,7,10-Tetraazacyclododecane-1,4,7,10-tetrayl)-tetraacetic acid (DOTA) chelator that can be loaded with radionuclides, since they were initially designed for radio-pharmaceutical applications (Fig. 1A) (29). The recognition

motifs coupled to oligoproline backbones yielded monovalent agonists/antagonists with the recognition motif in different distances to the DOTA chelator (30) and bivalent agonists/antagonist with 10-, 20-, and 30-Å distance between recognition motifs [(30, 31); see *SI Appendix*, Fig. 1 for characterization of previously unpublished ligands]. In addition, hybrid compounds with the agonist and the antagonist separated by 10, 20, and 30 Å were used (31). The schematic structure and nomenclature of the studied compounds are given in Fig. 1.

### Bivalent Ligands with 20- and 30-Å Distance Induce Dimerization.

Dimerization of GRPR was measured by coexpressing an NLuc-tagged and a Cherry-tagged GRPR (Fig. 2A). Bringing these two receptors in close proximity on the plasma membrane by dimerization leads to bioluminescence resonance energy transfer [BRET (32)]. No increase in the BRET signal was observed when cells were stimulated with AMBA or RM1, our reference compounds, indicating that these two compounds do not influence the oligomerization status of GRPR. This was also observed when a single agonist or antagonist was bound to an oligoproline backbone (Fig. 2B and C). However, stimulation with the 20- and 30-Å ligands (agonists, antagonists, and hybrids) resulted in an increase of the BRET signal within minutes, indicating dimerization (Fig. 2D–F). For hybrid and antagonistic bivalent ligands, saturation was reached after 1 to 3 min and for bivalent agonists within 10 min. As a control, we also used a GRPR mutant (GRPR-R288A-NLuc) that was previously shown to be unable to bind to ligands (33, 34). No dimerization was observed with this mutant, indicating that ligand binding is necessary for dimerization (*SI Appendix*, Fig. 2A). These different kinetics might be related to the internalization of the receptors stimulated by agonists. We also observed that the BRET signal for the bivalent hybrids and the antagonist with 30-Å distance is lower. Nevertheless, these values (kinetics and signal strength) should not be compared directly, since BRET signals depend on the distance and relative arrangement between BRET donor and acceptor, which are unknown. Stimulating cells with bivalent ligands at high concentrations can lead to “high-dose inhibition,” in which a bivalent ligand recruits only one receptor molecule due to saturation of receptors (35). However, we do not see a decrease in the dimerization signal at higher-ligand concentrations (10 μM), indicating that high-dose inhibition does not occur in our experimental setting (*SI Appendix*, Fig. 2B). The 10-Å bivalent ligands, on the other hand, did not induce a substantial change in the BRET ratio. These results indicate that the 20- and 30-Å ligands can induce receptor dimerization by “catching” the receptors on the plasma membrane and forcing them into close proximity. Conclusively, a distance of 20 and 30 Å between the ligands is suitable for accessing the binding pockets of two GRPR molecules at the same time, while 10 Å is too short to allow the concurrent interaction with two receptors.

**Recruitment of Adaptor Proteins to Activated GRPR.** Since GRPR homodimerization has not been reported, we were interested to find if our dimer-inducing ligands can also influence the balance between the receptor signaling pathways (i.e., induce biased signaling). Signaling bias can arise at the level of the ligand, the receptor, or the cell (6). As we are, in this work, exclusively interested in the effect of the ligands, we recorded time-resolved recruitment of adaptor proteins (G proteins, arrestins, and G protein-coupled receptor kinases [GRKs]) as a measure of their ability to alter receptor signaling. These assays are either based on enzyme complementation [split NanoLuc (36)] or BRET (37) (*SI Appendix*, Fig. 3B–D). With this strategy, we reduce the possible influence of the cell type that we would include by measuring downstream activity such as Erk phosphorylation or Ca<sup>2+</sup> production.

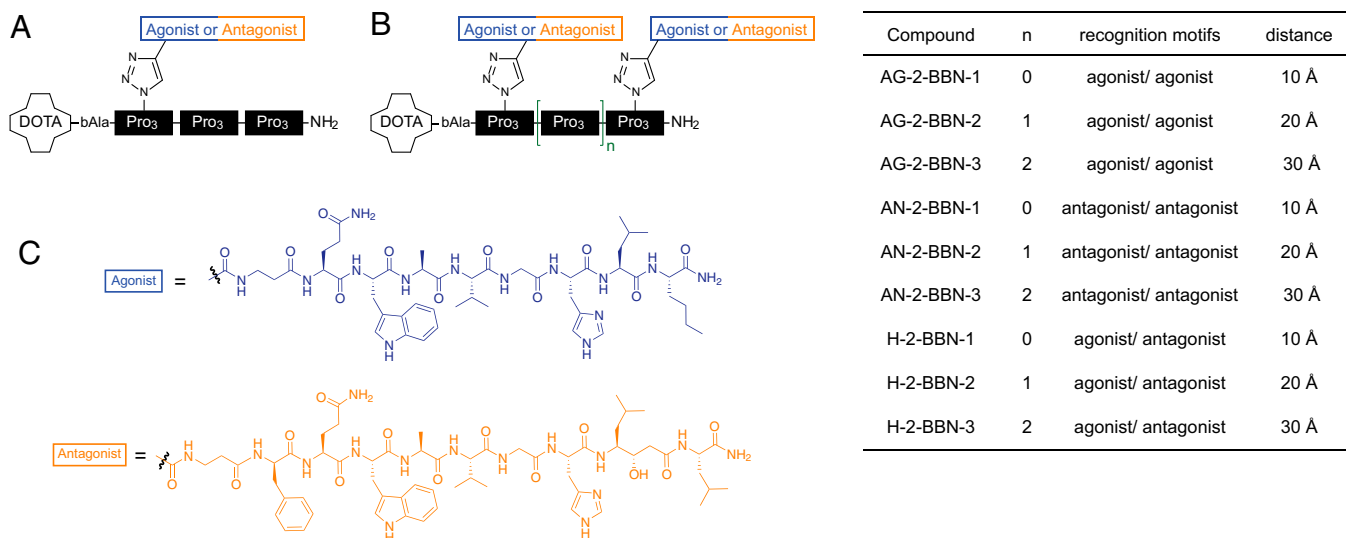


**Fig. 1.** Overview of used compounds. (A) AG-1-BBN-1 as an example for a monovalent compound. All monovalent compounds contain three blocks of three prolines. Agonists/antagonists were coupled to block 1, 2, or 3. (B) Bivalent ligands consist of two to four oligoproline blocks. The first ligand is always attached to block 1. The second ligand is linked to block 2, 3, or 4, resulting in bivalent ligands with a distance of 10, 20, and 30 Å between recognition motifs. Nomenclature and distances are given on the right side. (C) Chemical structures of the agonist (AMBA) and the antagonist (RM1).

Data were acquired at different ligand concentrations between 0.001 and 5 μM. Time-resolved data for the reference compound AMBA is shown in Fig. 3; data for all other ligands is shown in *SI Appendix, Fig. 4*. For measuring Gαq recruitment, we used a recently published BRET assay based on engineered Gα proteins (37). These probes provide an excellent signal-to-noise ratio but have the disadvantage that they are not released after binding. GRPR recruited the mGαq probe efficiently, reaching saturation within 10 min after stimulation with 1-μM agonist (Fig. 3A and *SI Appendix, Fig. 4A*).

GRPR interacts with both nonvisual arrestins (38). In the present study, β-arrestin-1 and β-arrestin-2 recruitment was measured using a split Nanoluc assay (39). A sharp increase in luminescence was observed after stimulation with high-agonist concentrations, reaching maximal signal within 3 min after stimulation (Fig. 3B and C and *SI Appendix, Fig. 4B and C*). The following decay of the signal was first steep and exponential but flattened after ~10 min to a slow decay. This biphasic reaction might be explained by the continuous synthesis/recycling/degradation of the receptor as described previously (36, 40).

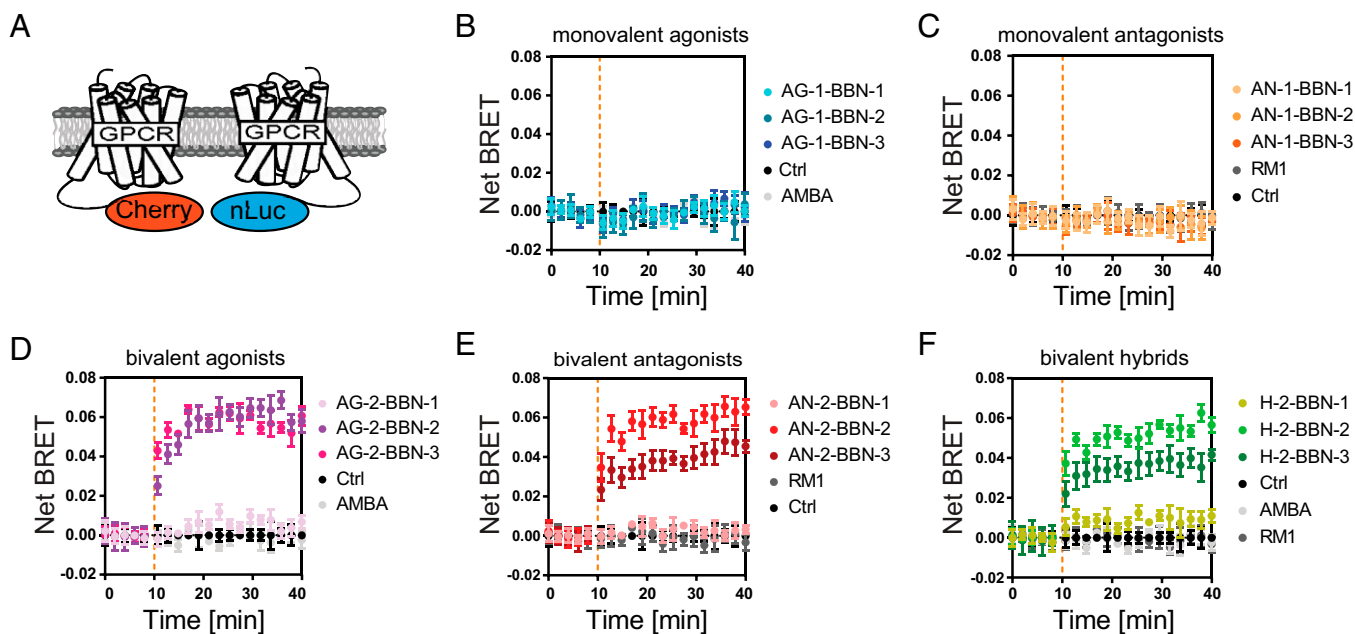


**Fig. 2.** Bivalent ligands with 20- and 30-Å distance induce receptor dimerization. (A) Dimerization was measured using HEK293 cells coexpressing an NLuc- and Cherry-tagged GRPR. (B and C) Monovalent agonists and antagonists were not able to induce receptor dimerization. (D–F) Bivalent agonists, antagonists, and hybrid compounds with 20- and 30-Å distance between ligands induced dimerization, whereas bivalent compounds with 10-Å distance failed to induce dimerization. The curves represent time-resolved measurements of one representative experiment out of three (mean ± SEM of triplicate). The orange dotted line indicates the time point of the ligand addition. Control (Ctrl): no ligand addition.

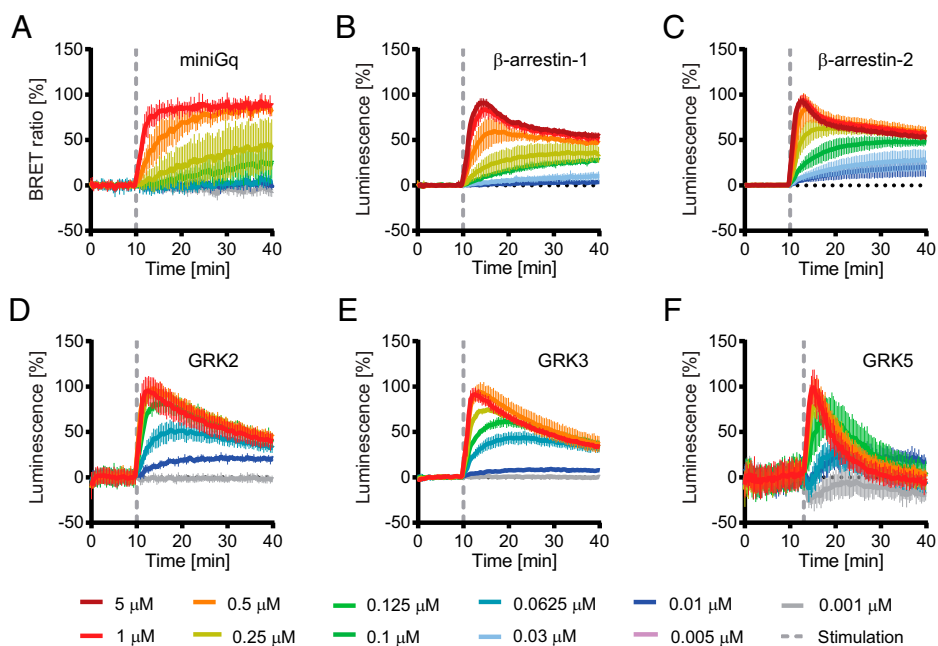


**Fig. 3.** Time-resolved measurement of adaptor protein recruitment to GRPR. Cells were stimulated with different concentrations of the reference compound AMBA at the indicated time point (dashed line). (A) BRET-based assay for miniGq recruitment. Nanoluciferase complementation assay for  $\beta$ -arrestin-1 (B),  $\beta$ -arrestin-2 (C), GRK2 (D), GRK3 (E), and GRK5 (F). Measurements for all other compounds are shown in *SI Appendix, Fig. 4*.

At lower-ligand concentrations, luminescence increased more slowly and reached saturation after  $\sim 10$  min.

GRKs are also known interaction partners of GPCRs. We used again split NanoLuc-based probes to measure GRK2, GRK3, and GRK5 recruitment to activated GRPR. GRK2/3 and GRK5 represent two branches of the GRK family that target different sequences leading to different phosphorylation patterns at the C-terminal tail of receptors (41). As for  $\beta$ -arrestins, a transient interaction with all three tested GRKs was observed (Fig. 3 D–F and *SI Appendix, Fig. 4 D–F*). Also, as in  $\beta$ -arrestins, maximal activation at high-ligand concentrations was reached within 3 min after stimulation, while at lower concentrations, the peak of the signal was shifted to later time points ( $>10$  min). Additionally, at lower concentrations, the recruitment of the adaptor proteins was no longer transient but remained at saturation during the whole time span of the assays.

**Effects on G $\alpha$ q Recruitment.** The data of the recruitment assays were then used to generate dose–response curves for all ligands (Fig. 4). From these dose–response curves, potencies (half maximal effective concentration,  $EC_{50}$ ) and efficacies ( $E_{max}$ ) of all drugs were obtained (Fig. 5). We observed a significantly increased efficacy toward miniGq recruitment for both dimer-inducing bivalent agonists (AG-2-BBN-2 and AG-2-BBN-3; Fig. 5A). The bivalent compound that is unable to induce receptor dimerization (AG-2-BBN-1) exhibits impaired miniGq potency and efficacy; this compound induced G-protein recruitment with an efficacy of only  $57 \pm 6\%$  and was therefore significantly less efficient than monovalent ligands and the bivalent compounds AG-2-BBN-2 and AG-2-BBN-3. Furthermore, AG-2-BBN-1 also exhibited a reduced potency for G-protein recruitment as compared with AMBA, AG-2-BBN-2, and AG-2-BBN-3.

Interestingly, all three monovalent agonists with oligoproline backbones show a clearly enhanced potency when compared to AMBA, whereas efficacies are similar to the values of AMBA. This suggests that the oligoproline backbone with its linker or the DOTA moiety may be in contact with the receptor and have an effect on Gq recruitment or lead to higher affinity.

**Effects on  $\beta$ -arrestin/GRK Potency and Efficacy.** We observed that the efficacies of all bivalent agonists toward  $\beta$ -arrestin-1 and  $\beta$ -arrestin-2 are similar to the reference agonist AMBA. This is contrast to the observed increased efficacy of the dimer-inducing compounds (AG-2-BBN-2 and AG-2-BBN-3) for miniGq recruitment. Monovalent agonists show slightly reduced efficacies toward  $\beta$ -arrestin-1 and  $\beta$ -arrestin-2. In contrast, we observed a clearly reduced potency for  $\beta$ -arrestin-2 recruitment after stimulation with the bivalent agonist with 20-Å distance (Fig. 5C). The monovalent agonists AG-1-BBN-2 and AG-1-BBN-3 showed both increased potencies for  $\beta$ -arrestin-2 recruitment. For GRK recruitment, we observed an increased potency with the dimer-inducing compound with 30-Å distance (AG-2-BBN-3) for GRK2/3 but not for GRK5 (Fig. 5 D–F). In addition, increased efficacies for GRK5 recruitment were measured for all monovalent compounds (Fig. 5F) that correlate with the increase in Gq potency (Fig. 5A).

**Implications for Signaling Balance.** The balance between different signaling pathways plays an important role in drug action (6). For better visualization of the observed effects toward effector recruitment, we use a two-dimensional bias plot to display efficacy and potency (Fig. 6; see *SI Appendix, Fig. 5* for a spider web representation). In our study, we use AMBA as reference agonist and consider it as unbiased. Our analysis reveals several interesting shifts in the signaling balance.

First, we observe that dimerization of GRPR leads to G-protein recruitment bias. Bivalent ligands show a clearly enhanced Gq efficacy with minor effects on  $\beta$ -arrestin and GRK2/3. In Fig. 6A, AG-2-BBN-2 and AG-2-BBN-3 are clearly shifted to the right of the graph, indicating G-protein bias (i.e., these compounds preferentially lead to G-protein recruitment over  $\beta$ -arrestin recruitment). Second, the nondimer-inducing bivalent ligand with 10-Å distance (AG-2-BBN-1) has lower potency and lower efficacy for Gq recruitment. This leads to a signaling shift toward  $\beta$ -arrestin and GRKs (Fig. 6B). The effector recruitment properties of AG-2-BBN-1 also clearly differ from those of the monovalent compounds. Finally, we also observe different recruitment between  $\beta$ -arrestin-1 and

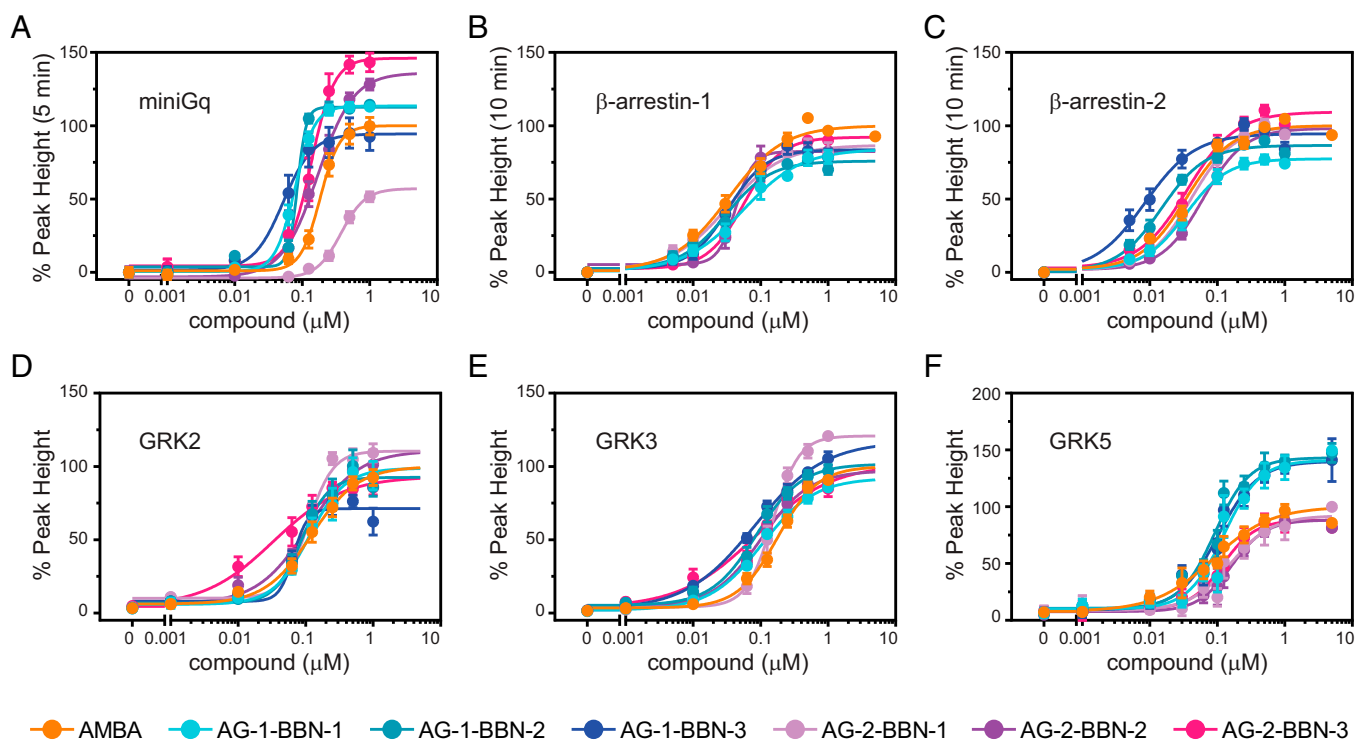


**Fig. 4.** Concentration–response curves reveal different efficacies and potencies for bivalent ligands. (A) miniGq, (B)  $\beta$ -arrestin-1, (C)  $\beta$ -arrestin-2, (D) GRK2, (E) GRK3, and (F) GRK5. Concentration–response curves were obtained from time-resolved experiments. Values represent the mean  $\pm$  SEM of at least nine replicates measured in at least three independent experiments.

$\beta$ -arrestin-2 for the two dimer-forming ligands. AG-2-BBN-2 (20 Å) has a lower potency toward  $\beta$ -arrestin-2. This leads to preference of AG-2-BBN-2 signaling toward  $\beta$ -arrestin-1 (yellow area in Fig. 6C). In contrast to that, the potencies of AG-2-BBN-3 (30 Å) toward  $\beta$ -arrestin-1 and  $\beta$ -arrestin-2 are similar to AMBA (orange area in Fig. 6C). AG-2-BBN-1, the bivalent agonist that does not induce receptor dimerization, did not exhibit a recruitment bias for any of the  $\beta$ -arrestins and recruited them with a similar potency to AMBA. Finally, we clustered the ligands according to their recruitment and dimerization potential. Data matrices were normalized, and *k*-means clustering was subsequently used to classify ligands. We observed that AG-2-BBN-1 forms a subtree with AMBA and that all monovalent ligands cluster together, as well as the bivalent agonists (SI Appendix, Fig. 6)

**Effects of Hybrid Compounds on Effector Recruitment.** We then also tested our hybrid compounds that are composed of an agonist and an antagonist. We observed for all compounds a clearly reduced efficacy for most assays (SI Appendix, Fig. 7). The mechanistic origin of this effect needs further investigation. Possible explanations are impaired internalization of the receptor or structural effects. Unfortunately, these low efficacies led to a reduced signal-to-noise ratio, which prevented us from getting concise potency data. Nevertheless, bivalent compounds with an agonist and antagonist could be promising when a reduced efficacy is desired.

## Discussion

In this work, we aimed to induce forced dimers of GRPR to overcome the limitations of its physiological signaling profile and thereby expand the possibilities for medicinal chemistry toward this receptor. The oligomerization state of GRPR under resting conditions is not known, but we could show that binding of monovalent ligands does not change the oligomerization

state. This does not exclude the idea that dimers or oligomers of GRPR may exist under resting conditions, as it was shown for several class A GPCRs, but they are probably not relevant for the activation process (42, 43).

Previous studies using bivalent ligands aimed to induce naturally occurring dimers and, therefore, mainly used flexible linkers to allow for a natural assembly of two receptors. In contrast, the oligoproline scaffold used in this work forms a stiff backbone that allows establishing defined distances between the attached ligands. Thus, binding of such more rigid bivalent ligands presumably reduces the mobility of attached GPCR dimers. We were able to induce dimers with oligoproline-based bivalent ligands at distance of 20 and 30 Å but not when the two recognition motifs were only 10 Å apart. This is in line with previous studies with flexible linkers that showed dimerization when ligands were spaced more than 15 Å (16, 17, 30).

We then investigated how these dimers may influence cellular signaling of GRPR by measuring recruitment of signaling partners. Surprisingly, we did not only observe effects of dimerization but also allosteric effects. In general, the effects of our ligands on Gq recruitment were larger than on  $\beta$ -arrestin/GRK, indicating that they preferably induce and stabilize the open receptor state that binds the G protein. On the other hand,  $\beta$ -arrestins are able to bind intermediate states of the opening process and thus are less sensitive to the allosteric effect of our ligands (44).

Interestingly, we observed opposite behavior on Gq efficacy of bivalent ligands depending on their ability to induce receptor dimers. Dimer-inducing compounds (at 20 to 30 Å) led to an increased efficacy, whereas the agonist with 10-Å distance had a reduced efficacy instead. This efficacy is independent of the receptor affinity of the ligand itself and depends mostly on the affinity of the adaptor protein to the receptor (45). Other works have shown that targeting GPCR homodimers with bivalent ligands often exhibit a decreased efficacy for G-protein

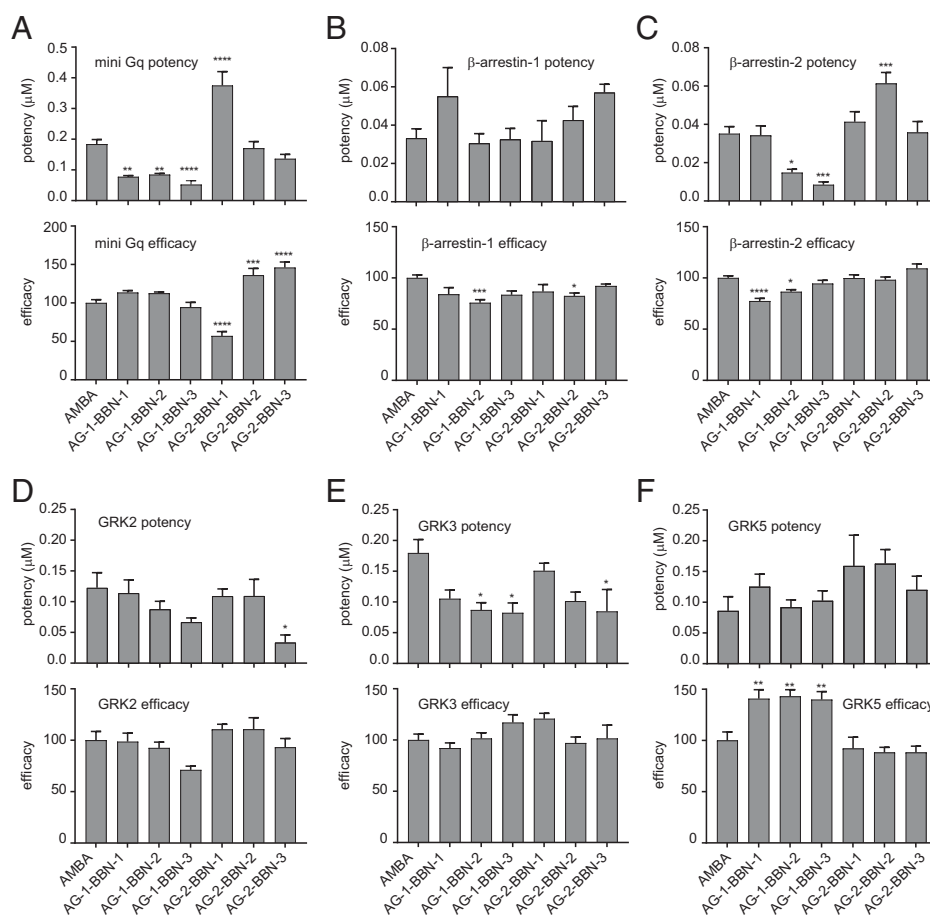


**Fig. 5.** Potency and efficacy. Potency and efficacy of tested ligands for recruitment of miniGq (A),  $\beta$ -arrestin-1 (B),  $\beta$ -arrestin-2 (C), GRK2 (D), GRK3 (E), and GRK5 (F). The asterisks indicate statistically significant differences to the reference compound AMBA. See *SI Appendix, Fig. 8* for pairwise comparisons. \* $P \leq 0.05$ , \*\* $P \leq 0.01$ , \*\*\* $P \leq 0.001$ , \*\*\*\* $P \leq 0.0001$ .

activation, becoming partial agonists or even antagonists (46, 47). In this regard, AG-2-BBN-2 and AG-2-BBN-3 differ from these common observations, suggesting that GRPR forced dimers may arrange in a different manner than natural homodimers, perhaps allowing positive cooperativity between two Gq adaptors. In contrast, the low efficacy of AG-2-BBN-1 is probably linked to decreased affinity of ligand-bound GRPR to Gq that is likely to result from a less favorable receptor active conformation. Furthermore, this ligand also showed reduced potency for Gq recruitment. In comparison to the efficacy, the potency depends on the affinity of the receptor for both the adaptor protein and the ligand. The 10-Å distance between two agonists in the polyproline scaffold is too short to recruit two receptors. Therefore, we speculate that one ligand occupies the receptor binding pocket, whereas the second ligand has an allosteric effect on the same receptor, for example, by interfering with the opening of the receptor during the activation process, thereby specifically preventing Gq recruitment but without affecting  $\beta$ -arrestin binding. Consequently, oligoprolines could be useful for delivering orthosteric and allosteric ligands simultaneously.

Interestingly, we observed a reduced potency of AG-2-BBN-2 toward  $\beta$ -arrestin-2, whereas its potency toward  $\beta$ -arrestin-1 is similar to AMBA. This difference could be caused by changes in potencies toward GRK2/3, resulting in different phosphorylation patterns that alter the competition of arrestins for the receptor. Even though these changes are currently relatively small, these compounds could be the basis to develop drugs that are able to switch the signaling balance of arrestin in vivo.

These effects were obtained with two identical ligands, but it is possible to use two different pharmacophores to amplify these effects. For example, we observed clearly reduced efficacies when we combined an agonist with antagonist (hybrid compounds). Even though the mechanistic origin of this effect is currently not clear, it clearly shows that the future combination of different ligands can further expand the possibilities of oligoprolines.

In summary, we have shown that rigid oligoproline backbones can be used to induce artificial GPCR dimers with altered signaling properties. In addition, we have shown that the stiff linkage of a second ligand at a short distance can also alter signaling properties, possibly through allosteric effects (Fig. 6D). Together, this work identifies oligoproline backbones as an interesting tool for the development of biased drugs for GPCRs that can be useful in the pharmaceutical industry and in scientific research (e.g., to develop ligands that can stabilize GPCR dimers for structural studies). Obvious candidates for such an approach are opioid and dopamine receptors for which biased ligands are in clinical trials (6).

## Materials and Methods

**Synthesis.** The recognition motifs were synthesized by regular solid-phase peptide synthesis and inserted into the oligoproline backbone by Cu(I)-catalyzed Huisgen's 1,3-dipolar cyclo-addition reactions ("click reaction"), as described before (31). They were purified by preparative reverse-phase high-performance liquid chromatography (HPLC) and characterized by mass spectrometry. The purity of all compounds was above 90% (30).

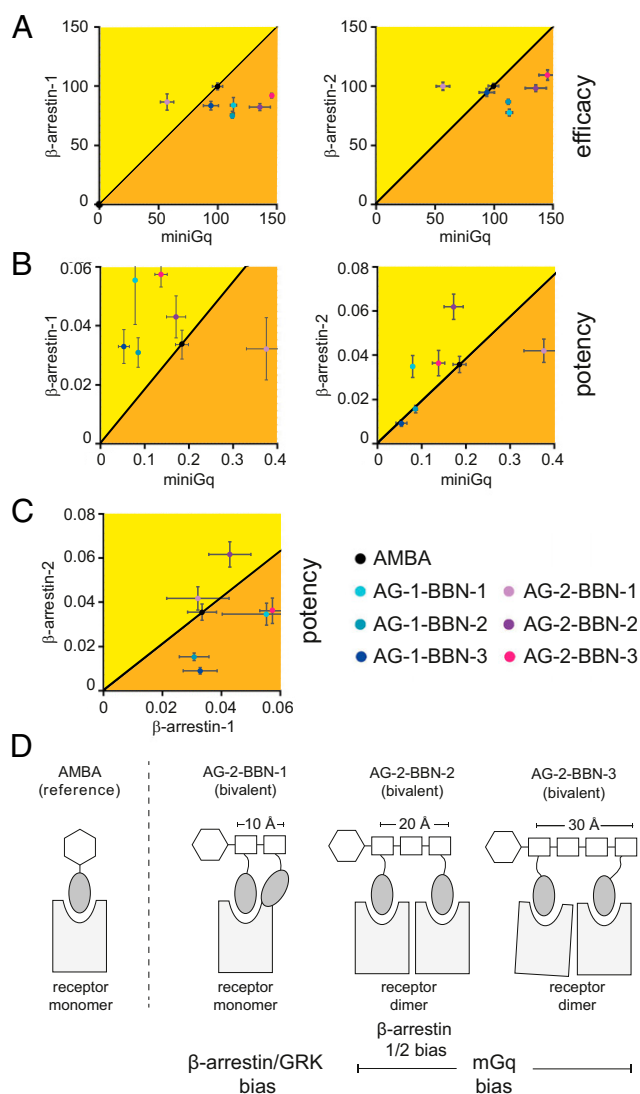


**Fig. 6.** Consequences for biased signaling. Pairwise comparison of recruitment assays. The reference compound AMBA (black) was considered as nonbiased or neutral. (A) The dimer-inducing compounds (AG-2-BBN-2/3) show higher-Gq efficacy than the reference compound, while the  $\beta$ -arrestin efficacy does not defer from the reference compound. (B) The nondimer-inducing bivalent compound (AG-2-BBN-1) shows a strong bias toward Gq signaling, while the dimer-inducing compounds show a bias toward  $\beta$ -arrestin signaling. (C) The dimer-inducing compounds showed different  $\beta$ -arrestin potency bias. (D) Schematic summary of obtained results.

**Cloning.** GRPR-expressing constructs with a C-terminal NLuc, 115, and Cherry tag were obtained by replacing the  $\beta$ 2-adrenergic receptor complementary DNA (cDNA) (B2AR) in pSI-AG10-B2AR-NLuc/115/Cherry with the coding region of human GRPR (39, 48). The cloning and characterization of 114- $\beta$ -arrestin-1/2 was described by Spillmann et al. (39). In brief, the C-terminal part of Nanoluciferase (114) was fused to the N terminus of  $\beta$ -arrestin-1/2, resulting in pSI-AA-114- $\beta$ -arrestin-1 and pSI-AA-114- $\beta$ -arrestin-2 (39, 49). For GRK, probe 114 was cloned at the C terminus of GRK2/3/5, resulting in pSI-AA-GRK2-114, pSI-AA-GRK3-114, and pSI-AA-GRK5-114 (SI Appendix, Fig. 3E). Probes for measurement of Gq recruitment were kindly provided by Nevin Lambert (Augusta University, Augusta, GA) (37).

**Cell Culture and Creation of Stable Cell Lines.** Human embryonic kidney (HEK293) cells (Merck, 85120602) or stable clones thereof were cultured in Dulbecco's Modified Eagle Medium (DMEM) with high glucose (No. 1-26F03-I, BioConcept) supplemented with 10% fetal bovine serum and 100 U/mL

penicillin/0.1  $\mu$ g/mL streptomycin (Sigma-Aldrich). Cells were propagated in a humidified atmosphere at 37  $^{\circ}$ C and 5% CO<sub>2</sub>.

Cell lines stably expressing GRPR-115 and either 114- $\beta$ -arrestin-1 or 114- $\beta$ -arrestin-2 were created from HEK293 cells by sequential transfection of pSI-AK1-GRPR-115 and pSI-AA-114- $\beta$ -arrestin-1/2 with Lipofectamin 3000 (Thermo Fisher Scientific) according to the manufacturer's recommendations. Stable cell lines were obtained by culturing cells in 5 mg/mL Geneticin (G418 sulfate, US Biological Life Sciences) or/and Zeocin (100  $\mu$ g/mL, Invitrogen).

**Dimerization Assays.** The dimerization assay was based on a NanoBRET system using pSI-AG10-GRPR-NLuc (donor) and pSI-AG10-GRPR-mCherry (acceptor). HEK293 cells were seeded in 6-well tissue culture plates at a density of  $1.5 \times 10^6$  cells per well 12 h prior to transfection. A total of 2  $\mu$ g DNA containing 90% carrier DNA and 5% of each construct was transfected using Lipofectamin 3000. Following transfection, the assay was performed according to the same protocol as the recruitment assays with a ligand concentration of 1  $\mu$ M. The measured emission wavelengths were 610 nm (mCherry) and 450 nm (NanoLuc). Then, the emission of these nonstimulated cells was measured in parallel and over the same time span as the emission of ligand-stimulated cells. The BRET ratio of nonstimulated cells (background) was subtracted from the BRET ratio of ligand-stimulated cells.

**Recruitment Assays.**  $\beta$ -arrestin recruitment was measured with cell lines expressing GRPR-115 and 114- $\beta$ -arrestin-1/2. GRK2/3/5 recruitment was measured by cotransfecting pSI-AG10-GRPR-115 and pSI-AA-GRK2-114, pSI-AA-GRK3-114, or pSI-AA-GRK5-114. These assays are based on split NanoLuc enzyme complementation (36). MiniGq recruitment was measured by a NanoBRET assay by coexpressing pSI-AG10-GRPR-NLuc as the BRET donor and venus-mGq as the BRET acceptor (37). For all recruitment assays,  $8 \times 10^6$  HEK293 cells were seeded in 10-cm culture dishes 12 h prior to transfection and then transiently transfected. Transfection was performed with Lipofectamin 3000 using 5  $\mu$ g total DNA. For GRK recruitment, the ratio of constructs was 1:1, while for miniGq recruitment, a donor:acceptor ratio of 3:1 was chosen. One day after transfection, the cells were reseeded in white 96-well microplates with clear bottoms (PerkinElmer) at a density of 80,000 cells per well and cultured for additional 24 h. For the assay, the culture medium was removed by inverting the microplate on a paper towel and replaced by 80  $\mu$ L assay buffer (20 mM HEPES in DMEM [high glucose, no phenol red, BioConcept]) containing furimazine according to manufacturer's recommendations (Promega, N2012). A removable white bottom was added to the microplate, and the baseline signal was measured in a PHERAstar FSX microplate reader (BMG Labtech) for 10 min at 37  $^{\circ}$ C. For the NanoBRET assays, emission was measured at 515 nm (Venus) and 410 nm (NanoLuc), while for the NanoLuc assay, the whole emission was measured from 100 to 1,000 nm. The ligand solutions for receptor stimulation were prepared in a separate 96-well microplate in assay buffer containing furimazine. A total of 20  $\mu$ L ligand solution was added to the cells directly after baseline measurement using a 96-channel bench-top pipette (Integra, Viaflo96), and the measurement was continued for at least 30 min. Each assay was done in triplicate and repeated three or more times.

**Data Analysis and Statistics of Concentration-Response Curves.** Analysis was performed using GraphPad Prism version 7.00 for Windows (GraphPad Software). For all datasets, the time-resolved curve of the nonstimulated control was subtracted from all other curves. These baseline-subtracted, time-resolved curves were then quantified. The area under the curve (AUC) was calculated by integration of the curve from the time point of stimulation until 20 min after stimulation. In addition, peak height at the time point of maximal activation with the highest concentration of the compound of interest was calculated for every concentration. These quantified values, AUC and peak height, were plotted against the compound concentration to receive the sigmoidal concentration-response curve. These were fitted by nonlinear regression using the "[Agonist] versus response - Variable slope (four parameters)" tool from GraphPad Prism. All dose-response curves of one assay were normalized to the efficacy (maximal activation) of the reference compound AMBA, which was set to 100%. Values represent the mean  $\pm$  SEM of at least three independent experiments with three replicate each. Potency (EC<sub>50</sub>) and efficacy were calculated by nonlinear regression of the concentration-response curves. The significance was calculated by ordinary one-way ANOVA followed by Tukey's multiple comparison test using GraphPad Prism version 7.00 for Windows, including an automatic outlier elimination.

**Data Availability.** Excel files with recruitment data have been deposited in the Open Science Framework (<https://osf.io/mh4bn/>) (50). All other study data are included in the article and/or SI Appendix.

**ACKNOWLEDGMENTS.** This work was supported by a Sinergia grant from the Swiss National Science Foundation (CRSII2\_160805) to M.B., X.D., H.W., and P.B. and a National Centre of Competence in Research (NCCR) Molecular Systems

Engineering (51NF40-182895) grant to G.F.X.S. We thank Dr. Nevin Lambert for providing plasmids, Dr. Gregor Cicchetti for critical reading of the manuscript, and Daniela Büttiker for help with data analysis and figure preparation.

1. M. J. Smit *et al.*, Pharmacogenomic and structural analysis of constitutive G protein-coupled receptor activity. *Annu. Rev. Pharmacol. Toxicol.* **47**, 53–87 (2007).
2. A. S. Hauser, M. M. Attwood, M. Rask-Andersen, H. B. Schiöth, D. E. Gloriam, Trends in GPCR drug discovery: New agents, targets and indications. *Nat. Rev. Drug Discov.* **16**, 829–842 (2017).
3. S. Rajagopal, K. Rajagopal, R. J. Lefkowitz, Teaching old receptors new tricks: Biasing seven-transmembrane receptors. *Nat. Rev. Drug Discov.* **9**, 373–386 (2010).
4. E. J. Whalen, S. Rajagopal, R. J. Lefkowitz, Therapeutic potential of  $\beta$ -arrestin- and G protein-biased agonists. *Trends Mol. Med.* **17**, 126–139 (2011).
5. J. W. Wisler *et al.*, A unique mechanism of beta-blocker action: Carvedilol stimulates beta-arrestin signaling. *Proc. Natl. Acad. Sci. U.S.A.* **104**, 16657–16662 (2007).
6. J. S. Smith, R. J. Lefkowitz, S. Rajagopal, Biased signalling: From simple switches to allosteric microprocessors. *Nat. Rev. Drug Discov.* **17**, 243–260 (2018).
7. T. Kenakin, Biased receptor signaling in drug discovery. *Pharmacol. Rev.* **71**, 267–315 (2019).
8. G. Milligan, R. J. Ward, S. Marsango, GPCR homo-oligomerization. *Curr. Opin. Cell Biol.* **57**, 40–47 (2019).
9. K. Kaupmann *et al.*, GABA(B)-receptor subtypes assemble into functional heteromeric complexes. *Nature* **396**, 683–687 (1998).
10. J. González-Maeso *et al.*, Identification of a serotonin/glutamate receptor complex implicated in psychosis. *Nature* **452**, 93–97 (2008).
11. A. Manglik *et al.*, Crystal structure of the  $\mu$ -opioid receptor bound to a morphinan antagonist. *Nature* **485**, 321–326 (2012).
12. S. A. Gaitonde, J. González-Maeso, Contribution of heteromerization to G protein-coupled receptor function. *Curr. Opin. Pharmacol.* **32**, 23–31 (2017).
13. D. Calebiro *et al.*, Single-molecule analysis of fluorescently labeled G-protein-coupled receptors reveals complexes with distinct dynamics and organization. *Proc. Natl. Acad. Sci. U.S.A.* **110**, 743–748 (2013).
14. M. Erez, A. E. Takemori, P. S. Portoghese, Narcotic antagonistic potency of bivalent ligands which contain beta-naltrexamine. Evidence for bridging between proximal recognition sites. *J. Med. Chem.* **25**, 847–849 (1982).
15. P. S. Portoghese *et al.*, Opioid agonist and antagonist bivalent ligands as receptor probes. *Life Sci.* **31**, 1283–1286 (1982).
16. A. H. Newman, F. O. Battiti, A. Bonifazi, 2016 Philip S. Portoghese medicinal chemistry lectureship: Designing bivalent or bitopic molecules for G-protein coupled receptors. The whole is greater than the sum of its parts. *J. Med. Chem.* **63**, 1779–1797 (2020).
17. C. Hiller, J. Kühhorn, P. Gmeiner, Class A G-protein-coupled receptor (GPCR) dimers and bivalent ligands. *J. Med. Chem.* **56**, 6542–6559 (2013).
18. S. Dobitz, M. R. Aronoff, H. Wennemers, Oligoprolines as molecular entities for controlling distance in biological and material sciences. *Acc. Chem. Res.* **50**, 2420–2428 (2017).
19. U. Lewandowska *et al.*, Hierarchical supramolecular assembly of sterically demanding  $\pi$ -systems by conjugation with oligoprolines. *Angew. Chem. Int. Ed. Engl.* **53**, 12537–12541 (2014).
20. M. Uhlén *et al.*, Proteomics. Tissue-based map of the human proteome. *Science* **347**, 1260419 (2015).
21. D. Xiao, J. Wang, L. L. Hampton, H. C. Weber, The human gastrin-releasing peptide receptor gene structure, its tissue expression and promoter. *Gene* **264**, 95–103 (2001).
22. C. Severi *et al.*, Different receptors mediate the action of bombesin-related peptides on gastric smooth muscle cells. *Am. J. Physiol.* **260**, G683–G690 (1991).
23. R. Roesler, G. Schwartzmann, Gastrin-releasing peptide receptors in the central nervous system: Role in brain function and as a drug target. *Front. Endocrinol. (Lausanne)* **3**, 159 (2012).
24. D. B. Cornelio, R. Roesler, G. Schwartzmann, Gastrin-releasing peptide receptor as a molecular target in experimental anticancer therapy. *Ann. Oncol.* **18**, 1457–1466 (2007).
25. M. Bologna, C. Festuccia, P. Muzi, L. Biordi, M. Ciomei, Bombesin stimulates growth of human prostatic cancer cells in vitro. *Cancer* **63**, 1714–1720 (1989).
26. J. Pinski, A. V. Schally, G. Halmos, K. Szepeshazi, Effect of somatostatin analog RC-160 and bombesin/gastrin releasing peptide antagonist RC-3095 on growth of PC-3 human prostate-cancer xenografts in nude mice. *Int. J. Cancer* **55**, 963–967 (1993).
27. R. Mansi *et al.*, Evaluation of a 1,4,7,10-tetraazacyclododecane-1,4,7,10-tetraacetic acid-conjugated bombesin-based radioantagonist for the labeling with single-photon emission computed tomography, positron emission tomography, and therapeutic radionuclides. *Clin. Cancer Res.* **15**, 5240–5249 (2009).
28. L. E. Lantry *et al.*,  $^{177}\text{Lu}$ -AMBA: Synthesis and characterization of a selective  $^{177}\text{Lu}$ -labeled GRP-R agonist for systemic radiotherapy of prostate cancer. *J. Nucl. Med.* **47**, 1144–1152 (2006).
29. E. W. Price, C. Orvig, Matching chelators to radiometals for radiopharmaceuticals. *Chem. Soc. Rev.* **43**, 260–290 (2014).
30. S. Dobitz *et al.*, Distance-dependent cellular uptake of oligoproline-based homobivalent ligands targeting GPCRs—An experimental and computational analysis. *Bioconjug. Chem.* **31**, 2431–2438 (2020).
31. C. Kroll *et al.*, Hybrid bombesin analogues: Combining an agonist and an antagonist in defined distances for optimized tumor targeting. *J. Am. Chem. Soc.* **135**, 16793–16796 (2013).
32. S. Angers *et al.*, Detection of beta 2-adrenergic receptor dimerization in living cells using bioluminescence resonance energy transfer (BRET). *Proc. Natl. Acad. Sci. U.S.A.* **97**, 3684–3689 (2000).
33. T. Nakagawa *et al.*, Identification of key amino acids in the gastrin-releasing peptide receptor (GRPR) responsible for high affinity binding of gastrin-releasing peptide (GRP). *Biochem. Pharmacol.* **69**, 579–593 (2005).
34. M. Akesson, E. Sainz, S. A. Mantey, R. T. Jensen, J. F. Battey, Identification of four amino acids in the gastrin-releasing peptide receptor that are required for high affinity agonist binding. *J. Biol. Chem.* **272**, 17405–17409 (1997).
35. F. Mac Gabhann, A. S. Popel, Dimerization of VEGF receptors and implications for signal transduction: A computational study. *Biophys. Chem.* **128**, 125–139 (2007).
36. A. S. Dixon *et al.*, NanoLuc complementation reporter optimized for accurate measurement of protein interactions in cells. *ACS Chem. Biol.* **11**, 400–408 (2016).
37. Q. Wan *et al.*, Mini G protein probes for active G protein-coupled receptors (GPCRs) in live cells. *J. Biol. Chem.* **293**, 7466–7473 (2018).
38. G. S. Kroog, X. Jian, L. Chen, J. K. Northup, J. F. Battey, Phosphorylation uncouples the gastrin-releasing peptide receptor from G(q). *J. Biol. Chem.* **274**, 36700–36706 (1999).
39. M. Spillmann *et al.*, New insights into arrestin recruitment to GPCRs. *Int. J. Mol. Sci.* **21**, 4949 (2020).
40. R. Irannejad *et al.*, Conformational biosensors reveal GPCR signalling from endosomes. *Nature* **495**, 534–538 (2013).
41. K. N. Nobles *et al.*, Distinct phosphorylation sites on the  $\beta(2)$ -adrenergic receptor establish a barcode that encodes differential functions of  $\beta$ -arrestin. *Sci. Signal.* **4**, ra51 (2011).
42. J. A. Hern *et al.*, Formation and dissociation of M1 muscarinic receptor dimers seen by total internal reflection fluorescence imaging of single molecules. *Proc. Natl. Acad. Sci. U.S.A.* **107**, 2693–2698 (2010).
43. A. Tabor *et al.*, Visualization and ligand-induced modulation of dopamine receptor dimerization at the single molecule level. *Sci. Rep.* **6**, 33233 (2016).
44. L. M. Wingler *et al.*, Angiotensin analogs with divergent bias stabilize distinct receptor conformations. *Cell* **176**, 468–478.e11 (2019).
45. M. S. Salahudeen, P. S. Nishtala, An overview of pharmacodynamic modelling, ligand-binding approach and its application in clinical practice. *Saudi Pharm. J.* **25**, 165–175 (2017).
46. O. Russo *et al.*, Synthesis of specific bivalent probes that functionally interact with 5-HT(4) receptor dimers. *J. Med. Chem.* **50**, 4482–4492 (2007).
47. M. Nimczick *et al.*, Synthesis and biological evaluation of bivalent cannabinoid receptor ligands based on hCB<sub>2</sub>R selective benzimidazoles reveal unexpected intrinsic properties. *Bioorg. Med. Chem.* **22**, 3938–3946 (2014).
48. M. Mansouri *et al.*, Highly efficient baculovirus-mediated multigene delivery in primary cells. *Nat. Commun.* **7**, 11529 (2016).
49. A. Kriz *et al.*, A plasmid-based multigene expression system for mammalian cells. *Nat. Commun.* **1**, 120 (2010).
50. P. Berger, Oligoproline-based ligands for GRPR. Open Science Framework. <https://osf.io/mh4bn/>. Deposited 6 October 2021.